

RESEARCH

Open Access



# Baculovirus displaying SARS-CoV-2 spike RBD promotes neutralizing antibody production in a mouse model

Mohamed A. Wahba<sup>1</sup>, Dina Mofed<sup>1</sup>, Doaa A. Ghareeb<sup>2</sup>, Jihad I. Omran<sup>1</sup> and Tamer Z. Salem<sup>1,3,4\*</sup>

## Abstract

**Background** There is always a need for a safe and efficient vaccine platform, especially when facing a pandemic such as COVID-19. Most of the SARS-CoV-2-based vaccines are based on the full spike protein, which is presented as a trimerized protein, and many viral vector vaccines express the spike protein into the host cells and do not display it on virus surfaces. However, the spike receptor-binding domain (RBD)-based vaccines are efficient and are currently under investigation and clinical trials.

**Methodology** In this study, we are testing the efficacy of the RBD displayed on a baculovirus as a mean to formulate a safe and stable carrier to induce the immune system against SARS-CoV-2. Therefore, two pseudotyped baculoviruses were constructed to display the RBD, AcRBD-sfGFP-64, and AcRBD-sfGFP-V, using two different displaying strategies based on gp64 and VSV-G envelope glycoproteins, from *Autographa californica* multiple nucleopolyhedrovirus (AcMNPV) and vesicular stomatitis virus (VSV), respectively. BALB/C mice were immunized with the pseudotyped baculoviruses in a dose-optimized manner. Dot blot and Western blot were used to screen and validate the polyclonal antibodies' specificity to the SARS-CoV-2 RBD. A plaque reduction neutralization test (PRNT) was used to measure the sera neutralization capacity against a SARS-CoV-2 wild-type isolate from Egypt. ELISA was used to quantify certain cytokines for the assessment of the immune response.

**Result** The outcome of our investigation showed that the monomeric RBD proteins were properly displayed on baculovirus and efficiently triggered the mouse immune system. The produced sera efficiently neutralized about 50% of SARS-CoV-2 in more than 100-fold serum dilution. The immunized mice showed a significant increase ( $p < 0.01$ ) in the levels of IL-2 and IFN- $\gamma$  and a significant decrease ( $p < 0.01$ ) and ( $p < 0.001$ ) in the levels of IL-4 and IL-10, respectively, which suggest that AcRBD-sfGFP-64 and AcRBD-sfGFP-V induce Th1 cellular immune response.

**Conclusion** The produced recombinant viruses can induce the immune response without adjuvant, which needs dose optimization and further stability tests. Neutralizing antibodies were induced without affecting the health of immunized mice. Th1 response can be attainable through the system, which is of great benefit in SARS CoV-2 infection and the system can be tested for future applications including vaccine development and polyclonal antibody production.

**Keywords** SARS CoV-2, Pseudotyped virus, Baculovirus, Neutralizing antibody, AcMNPV, RBD, Spike

\*Correspondence:

Tamer Z. Salem  
tsalem@zewailcity.edu.eg

<sup>1</sup> Molecular Biology and Virology lab, Biomedical Sciences program, UST, Zewail City of Science and Technology, October Gardens, 6th of October City, Giza 12578, Egypt

<sup>2</sup> Bio-screening and preclinical trial lab, Biochemistry Department, Faculty of Science, Alexandria University, P.O. Box 21511, Alexandria, Egypt

<sup>3</sup> Department of Microbial Genetics, Agricultural Genetic Engineering Research Institute (AGERI), ARC, Giza 12619, Egypt

<sup>4</sup> National Biotechnology Network of Expertise (NBNE), Academy of Science Research and Technology (ASRT), Cairo 11334, Egypt

## Background

Emerging infectious disease refers to the recent appearance of unknown or previously known pathogens [1]. Emerging viruses can be dangerous, especially with the lack of the necessary equipment and facilities. The lack of biosafety-level facilities in many developing countries has a negative impact on studies related to emerging viruses [2]. Moreover, the need for biocontainment infrastructure to produce live-attenuated or inactivated vaccines imposes a major limitation [3]. An alternative safe platform that can be adaptable and versatile is highly needed [3]. The current pandemic of COVID-19 showed us how low-income countries suffered greatly during this crisis as 15.9% of their populations received at least a single dose compared to 65.5% of the total worldwide vaccination [4]. Baculovirus may hold significant potential for the current and future pandemics in terms of safety, immunogenicity, and its versatility to be tailored against various pathogens. Baculovirus is an insect virus that has been recognized as a non-human viral vector. The double-stranded DNA *Autographa californica* multiple nucleopolyhedrovirus (AcMNPV) is the prototype of baculoviruses that has been used extensively to produce eukaryotic complex proteins [5]. AcMNPV poses many advantages over other viral vectors, including the ease of production with a high titer, the ability to simultaneously deliver multiple genes, the transduction ability to many mammalian cells, and its non-pathogenicity non-replicative nature in humans [6–8]. The primary envelope glycoprotein gp64 is the most abundant envelope protein and is essential for both insect cell infection and mammalian cell transduction [9]. Many researchers have been able to display many proteins such as glutathione-S-transferase, HIV GP120 protein, rubella virus envelope protein, and synthetic IgG-binding domains on the baculovirus membrane [10–12]. On the other hand, VSV-G and HA proteins can be displayed on baculovirus independently from gp64 protein [11, 13, 14]. Usually, the display sequences are derived from gp64 and VSV-G from three main components: the signal sequence, the transmembrane domain, and the cytoplasmic domain [15]. Indeed, baculovirus is an excellent immunogen, as it triggers proinflammatory cytokines via the TLR9 pathway. This inherent property is due to a highly abundant structurally distinct unmethylated CpG motif in its DNA [16]. The adjuvant property plays a major role in dendritic cell maturation, followed by the induction of both cellular and humoral immune responses [15, 17]. Moreover, mammalian promoters such as the CMV promoter or the display by other membrane fusion proteins like VSV-G or human endogenous retrovirus (HERV) envelope protein can enhance transduction efficacy and immune response [18–20]. Nevertheless, the displayed antigen on

baculoviral will not necessarily require such modifications, as it will confer potent humoral and cellular immunity upon administration [17].

The beta coronavirus family encompasses the causative agent of COVID-19 severe acute respiratory syndrome virus (SARS CoV-2) along with the Middle East respiratory syndrome virus (MERS-CoV) and severe acute respiratory syndrome virus (SARS-CoV) [21, 22]. SARS CoV-2 is a single-stranded RNA virus (~30 kb) with four structural proteins membrane (M), envelope (E), spike (S), and nucleocapsid (N) proteins [23]. The ACE2 binding and fusion events are organized by the S protein. It has two main subunits the S1 and S2 that are cleaved during its biosynthesis by the host cell furin proteases. The virus binding is catalyzed by the S1 subunit when interacting with host cell receptor ACE2 through the receptor-binding domain (RBD) followed by the fusion with the cell membrane via the S2 subunit fusion peptide [23, 24]. Currently, most of the vaccine arsenal depends on the full S protein. However, the vaccine design based on the RBD may offer a better safety profile. Several studies reported abnormal protein splicing, and alternative polyadenylation (APA) events of the Spike protein were associated with adenovirus vector vaccine (ChAdOx1 nCoV-19) in vitro. The mechanism may lead to C-terminal truncation producing soluble spike protein and binding to endothelial cells via the ACE2 receptor, which might be the cause of thrombosis after an antibody attack to such a complex [25–28]. Therefore, vaccines based on the RBD, the most targeted region by the neutralizing antibodies will be of great value to the current pandemic [29]. The platform and the adjuvant other than the immunogen may shape the immune response differently. For instance, subunit vaccines may shift the balance of Th1/Th2 CD4+ T cell response [28, 30]. In addition, the currently most used vaccines such as mRNAs can induce more neutralizing antibodies while the adenovirus vector vaccine can promote specific cytotoxic T cells efficiently [31].

Researchers have put tremendous efforts to develop various RBD-based vaccines that are already in the pre-clinical and clinical trials. These vaccines are adopted in several systems and have different immune responses (summarized in supplementary data, Table 1). For example, BNT162b1 and ArCov carry SARS-CoV-2 RBD mRNA triggering the production of CD4+ and CD8+ cells and increasing the production of IFN- $\gamma$  and IL-2, resulting in enhancing Th1 immune response [32, 33]. Folded RBD-PreS fusion vaccine is based on the fusion of SARS-CoV2 “RBD with hepatitis B virus (HBV) antigen in N and C terminus and expressed in *Escherichia coli* expression system, which promotes the production of allergen-specific IgG responses (IgG1 and IgG 4) [34].

Also, the ZF2001 vaccine is an adjuvant based-protein subunit vaccine, which promotes Th1 cytokine production (IFN- $\gamma$ , IL-2) and Th2 cytokine production (IL-4), resulting in increasing Th1 and Th2 immune responses [35, 36]. A yeast-expressed RBD-based SARS-CoV-2 vaccine triggers the responses of CD4+ and CD8+ T cells resulting in the promotion of the Th1 cellular immune response [37]. Moreover, west china hospital has developed a recombinant RBD of SARS-CoV2 `spike protein expressed in the baculovirus expression system. It induces the production of IgM and IgG antibodies and enhances the levels of IFN- $\gamma$  and IL-4 from isolated lymphocytes, resulting in promoting Th1 and Th2 immune responses [38]. Moreover, Song and his colleagues have improved the mutant RBD vaccine expressed in the HIV-1 backbone, which induces the production of highly potent neutralizing antibodies against SARS-CoV-2 WT strain or their variants including Beta, Delta, Alpha, Iota, Kappa, or A.23.1 [39]. We considered the above-stated facts to ensure a safe vaccine platform of baculovirus that has no previous immunity in humans. This can be a useful tool with the increasing evidence of autoimmune disorders associated with COVID-19 and some of its vaccines [40].

In this work, we have selected baculovirus as a safe and efficient platform to display the monomeric spike receptor-binding domain (RBD) fused with a superfolder green fluorescent protein (RBD-sfGFP) as a tracking marker for the produced pseudovirus particles. The RBD-sfGFP fused protein was previously used in another study, and its binding capacity to ACE2 was already confirmed; hence, the 3D structure and function of the RBD are not affected by the sfGFP fusion [41]. The immunogenicity of the produced pseudotyped baculoviruses was assessed and discussed. The obtained sera showed neutralizing activity against a wild-type SARS CoV-2 with elevated Th1 response.

## Methods

### Cell lines

The *Spodoptera frugiperda*-Sf9 insect cell line (ATCC) was maintained in a monolayer at 26°C with an ExCell-420 insect medium (Sigma Aldrich, USA) supplemented with 10% fetal bovine serum (FBS) (Gibco, ThermoFisher Scientific, USA).

### SARS-CoV-2 RBD-sfGFP pseudotyped baculoviruses production

To produce SARS-CoV-2 pseudotyped baculoviruses, AcRBD-sfGFP-64 and AcRBD-sfGFP-V, the RBD-sfGFP fragment was cloned between gp64 mature domain (TM+CTD) and gp64 signal sequence or VSV-G mature domain (TM+CTD) and VSV-G signal, respectively.

Gp64 and VSV-G sequences were PCR amplified from AcMNPV genomic DNA and VSV-G from pCMV-VSV-G, a gift from Bob Weinberg (Addgene plasmid # 8454; <http://n2t.net/addgene:8454>; RRID: Addgene 8454), respectively. The gp64 and VSV-G signal sequences were cloned into pFastBac™ Dual vector using *Bam*HI-HF and *Eco*RI-HF. The mature domain of gp64 and VSV-G sequences were cloned in the same vector using *Xba*I and *Hind*III-HF. The RBD-sfGFP DNA fragment was PCR amplified from pcDNA3-SARS-CoV-2-S-RBD-sfGFP, a gift from Erik Procko (Addgene plasmid # 141184; <http://n2t.net/addgene:141184>; RRID: Addgene141184) and cloned using *Eco*RI-HF and *Xba*I between the signal sequence and mature domain of the gp64 and VSV-G. The recombinant vectors were authenticated by sequencing (supplementary). In addition, AcEGFP was previously constructed and used in this study as a control virus [42]. Another control baculovirus (AcDH10Bac) was prepared by transfecting Sf9 cells with DNA isolated from DH10Bac using Cellfectin II reagent (ThermoFisher, USA). The produced virus stocks of AcRBD-sfGFP-64, AcRBD-sfGFP-V, AcEGFP, and the control virus were purified by the Pierce™ Strong Anion Exchange Spin Column, Mini (ThermoFisher, USA).

### Virus quantification and verification by endpoint dilution, in-gel fluorescence, and transmission electron microscope

Virus stocks were tittered by the end-point dilution. In 96 well-plate, Sf9 cells were seeded at a density of  $2 \times 10^4$  cells/100 $\mu$ l. A 10-fold serial dilution of the virus stock was made from  $10^{-2}$  to  $10^{-9}$  and each dilution was plated in 12-well replicas. After seven days of infection, the infected wells were calculated by fluorescent microscope using a FITC filter (Olympus, Japan) [43]. In-gel fluorescence was used to confirm the fluorescent activity of the fused RBD-sfGFP protein, as described in [44]. For further confirmation and identification, transmission electron microscopy (TEM) was used to identify the structure of the purified AcRBD-sfGFP-64 ( $10^8$  pfu/ml) in the electron microscopy unit at Mansoura University. The purified AcRBD-sfGFP-64 ( $10^8$  pfu/ml suspension) was loaded on a carbon-coated Cu-grid (200 mesh) for 5 min at RT and negatively stained with 2% phosphotungstic acid for 3 min before air drying on a filter paper. The samples were examined using a transmission electron microscope (Jem -2100, USA) at 200 KeV.

### In vivo experiment

The mice were treated in accordance with the guidelines and policies of the National Institute of Health (NIH) animal care. All experiments were approved by the research ethics committee (IACUC#50-2S-1121) issued from the Pharmaceutical & Fermentation industries Development

center, SRTA-City. Twenty female BALB/C from 4- to 6-week-old mice were purchased from the National Research Center (NRC). The mice were kept in universal polypropylene cages and divided into four different groups for injection: AcRBD-sfGFP-64, AcRBD-sfGFP-V, AcEGFP, and phosphate-buffered saline (PBS) buffer each group ( $N=5$ ). Each group was assigned a different label according to different concentrations of baculovirus  $10^8$ ,  $10^9$ , and  $10^{10}$  PFU administered subcutaneously. The first injection was done after mixing the purified virus with complete Freund's adjuvant (Sigma-Aldrich, USA) except for the  $10^{10}$  PFU dose. After 2 weeks after the first dose, the booster doses with the same concentrations were injected by mixing with incomplete Freund's adjuvant (Sigma-Aldrich, USA). At the end of the month, the blood was harvested from the retro-orbital vein after local anesthesia. The anti-sera were screened by dot blot and western blot to confirm the display.

#### Dot blot and western blot

Dot blot and western blot were performed using the Amersham™ ECL Western Blotting and analysis system (GE Healthcare, Buckinghamshire UK). All reagents were prepared and adapted in 24-well plates to include 200  $\mu$ l of any reagent or antibody. First, 0.2  $\mu$ m nitrocellulose was cut into small circles in a 24-well plate and then incubated for 15 min with 3  $\mu$ l of AcRBD-sfGFP-64 and AcEGFP ( $\sim 3 \times 10^8$  PFU). All wells were blocked by soaking in 5% non-fat dry milk in PBS-T (PBS with Tween 20 0.1%) for 30 min at RT and washed twice with PBS-T. Primary antibodies (serum) were diluted 1:100 by dissolving in PBS-T and incubated for 30 min at RT before the membranes were washed thoroughly three times with PBS-T (3  $\times$  5 min) followed by incubation with secondary antibody conjugated with HRP (1:1000) for 30 min at RT and washed three times with PBS-T (15 min  $\times$  1, 5 min  $\times$  2), and once with PBS (5 min). Quickly, the detection reagent was added and the membrane was examined by ChemiDoc XRS+ (Bio-Rad, USA). In the positive control of the dot blot, the anti-gp64 antibody was used [AcV5] (Abcam, USA). For western blot, the blotting step was done on a nitrocellulose membrane (0.2  $\mu$ m) following the instructions of the Bio-Rad blotting protocol that took 2.5 h in 20V. The detection was conducted similar to the dot blot in which, the serum from  $10^{10}$  doses of AcRBD-sfGFP-V was used as the primary antibody and diluted at 1:100.

#### Plaque reduction neutralization test (PRNT)

This experiment was conducted at Nawah Scientific Co. (Al-Asmarat, Egypt) following the PRNT protocol described before [45]. The serum sample was 10-fold serially diluted and mixed with hCoV-19/Egypt/

NRC-03/2020 (Accession number on GSAID: EPI\_ISL\_430820) and then incubated along with the control untreated virus. Vero E6 was seeded in supplemented DMEM media and incubated for 24 h at 37 °C with 5% CO<sub>2</sub>. After the removal of culture media, 100  $\mu$ l of the sample was incubated with the cells for 1 hr at 37°C followed by adding 3 ml DMEM media and 2% agarose overlay and left to solidify before incubation at 37°C with 5% CO<sub>2</sub>. After 4 days, the plaques appeared and then a 10% formalin was added for 2 h and stained with 0.1% crystal violet, and plaques were recorded as % inhibition = viral count (un-treated) - viral count (treated)/viral count (untreated)  $\times$  100.

#### Estimation of the levels of IL-2, IL-4, IL-10, and IFN- $\gamma$ in isolated splenocytes

Spleens were isolated from dissected mice and homogenized into a single-cell suspension using PBS buffer, then filtered with 40- $\mu$ m Falcon™ Cell Strainers (fisher scientific, USA). The red blood cells were lysed by ammonium-chloride-potassium (ACK) lysing buffer (ThermoFisher, USA), followed by centrifugation for 5 min at 2000 RPM and removal of the supernatant. The cell pellets were washed with 100  $\mu$ l of ACK buffer 2–3 times to get a clear white pellet; finally, the cells were preserved in RPMI media supplemented with 10% FBS and 10% DMSO at  $-80^{\circ}$ C. The cells were thawed and then seeded overnight in 60 mm plates and harvested for total protein extraction using cComplete™ Lysis-M (Roche, Germany) following its protocol. IL-2, IFN- $\gamma$ , IL-4, and IL-10 levels were measured using ELISA kits following the manufacturer's instructions (Elabscience Biotechnology Inc, USA).

#### Data analysis

Pairwise *t* test was used to evaluate the significance of the cytokines ELISA readings performed with GraphPad Prism 8.0 (GraphPad Software, Inc., San Diego, CA).

## Results

#### Production of pseudotyped baculovirus displaying SARS CoV-2 RBD fused with sfGFP

The signal sequence, TM, and CTD of Gp64 and VSV-G were used to display RBD-sfGFP on baculovirus; viruses were named AcRBD-sfGFP-64 and AcRBD-sfGFP-V, respectively (Fig. 1a). To confirm the morphology of the produced virus, AcRBD-sfGFP-64 was validated by TEM, which demonstrated an intact rod shape structure of the budded virus (BV) 30–70 nm in diameter and 200–400 nm in length (Fig. 1b). The main aim of sfGFP incorporation is to localize the RBD hence the fluorescence image of the infected Sf9 cells with AcRBD-sfGFP-64 showed fluorescence foci, and around the periphery of the cell, which is an expected pattern for transmembrane

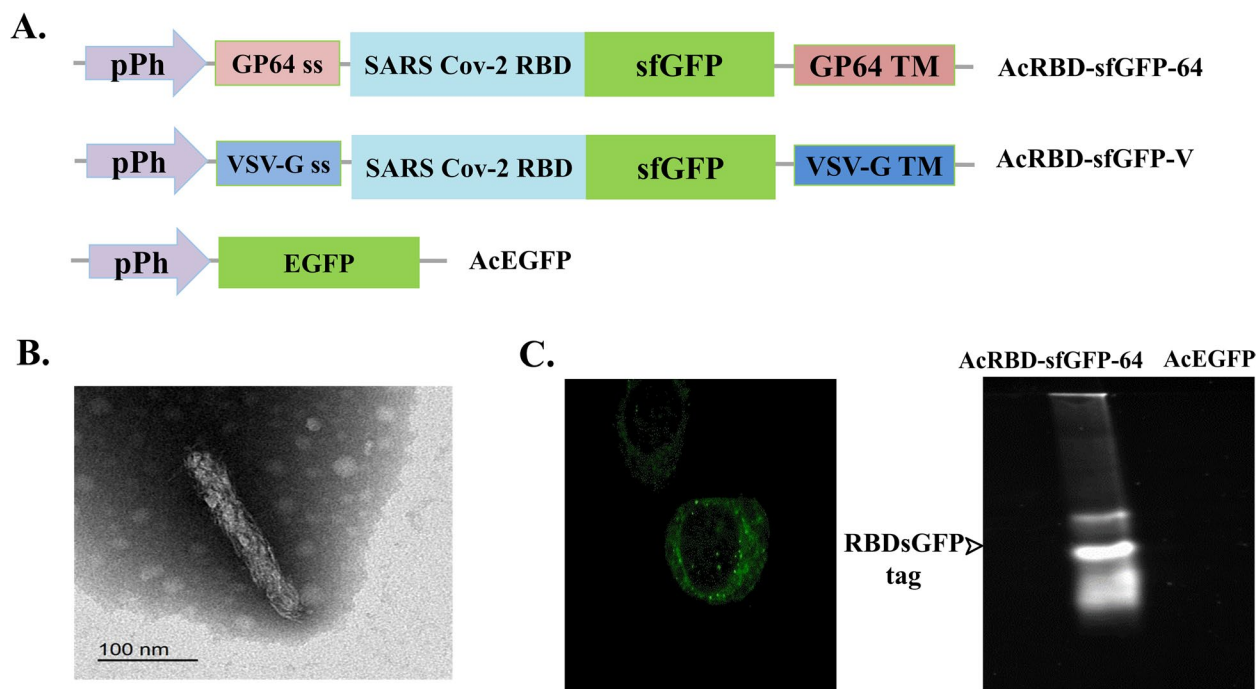


**Fig. 1** Production of pseudotyped baculovirus displaying the RBD-sfGFP based on gp64 and VSV G-proteins. **a** Schematic map for bacmid constructs; all constructs were under polyhedrin promoter (Pph). **b** TEM of AcRBD-sfGFP-64 showing a rod-shaped budded virus (BV) 30–70 nm in diameter and 200–400 nm in length. **c** Validation of the function of the displayed protein by showing fluorescence on Sf9 cell periphery and ER using fluorescence microscopy under 60 $\times$  objective and with in-gel fluorescence

proteins (Fig. 1c). In addition, the in-gel fluorescence of AcRBD-sfGFP-64 showed fluorescent bands indicating that the RBD-sfGFP is part of the virus in comparison to the control virus AcEGFP, which showed no fluorescent bands (Fig. 1c). Viruses were purified by anion exchange chromatography and viruses' titers after endpoint dilution was  $1.47 \times 10^{11}$ ,  $1.23 \times 10^{11}$ , and  $1 \times 10^{11}$  Pfu/ml for AcRBD-sfGFP-64, AcRBD-sfGFP-V, and AcEGFP, respectively.

#### Screening of mice Sera against anti-RBD polyclonal antibodies

Our aim in this experiment was to prove the capability of the monomeric RBD to be recognized by and trigger the immune system and to optimize the dose of baculovirus injection as many previous studies used inconsistent doses. Mice were in good health during the 30-day experiment without mortality and the sera collected were preserved at  $-20^{\circ}\text{C}$  until used. AcRBD-sfGFP-64, AcRBD-sfGFP-V, and AcEGFP sera of different injection doses;  $10^8$ ,  $10^9$ , and  $10^{10}$  PFU were tested by dot blot in which the antigens either AcEGFP or AcRBD-sfGFP-64 were blotted on membranes as seen in (Fig. 2A). The antibody that can optimally bind both AcEGFP and AcRBD-sfGFP-64 was detected at  $10^{10}$  PFU of AcRBD-sfGFP-V subcutaneous serum without any

adjuvant (Fig. 2A). However, the dot blot method could not distinguish whether the polyclonal antibodies in the serum were specific to the RBD or not. Therefore, western blot analysis was performed for AcRBD-sfGFP-64, AcRBD-sfGFP-V, and the AcDH10Bac to differentiate the RBD-sfGFP specific band from other bands that can be targeted by the polyclonal antibodies. Since Gp64 is the major envelope glycoprotein of AcMNPV BV, it is expected to be seen at around the 60–72 kDa band. Moreover, the fused RBD-sfGFP protein size was estimated to be 51 kDa using the protein molecular weight software tool ([Bioinformatics.org](http://Bioinformatics.org)). Interestingly, only two distinguished bands corresponding to gp64 around the size of 62–70 kDa and to RBD-sfGFP around 51–62 kDa for AcRBD-sfGFP-64 and AcRBD-sfGFP-V samples were shown, while only a single band corresponding to gp64 was shown for the AcDH10Bac (Fig. 2b). Even though, the AcMNPV BV envelope contains other proteins than gp64; they were not detected. Furthermore, the intensity of the RBD-sfGFP band of the AcRBD-sfGFP-V sample was more intense than the AcRBD-sfGFP-64 sample; the same was observed with the gp64 band (Fig. 2b L 2 & 3). Interestingly, the gp64 band was similar in both AcRBD-sfGFP-V and AcDH10Bac but decreased in AcRBD-sfGFP-64 (Fig. 2b).

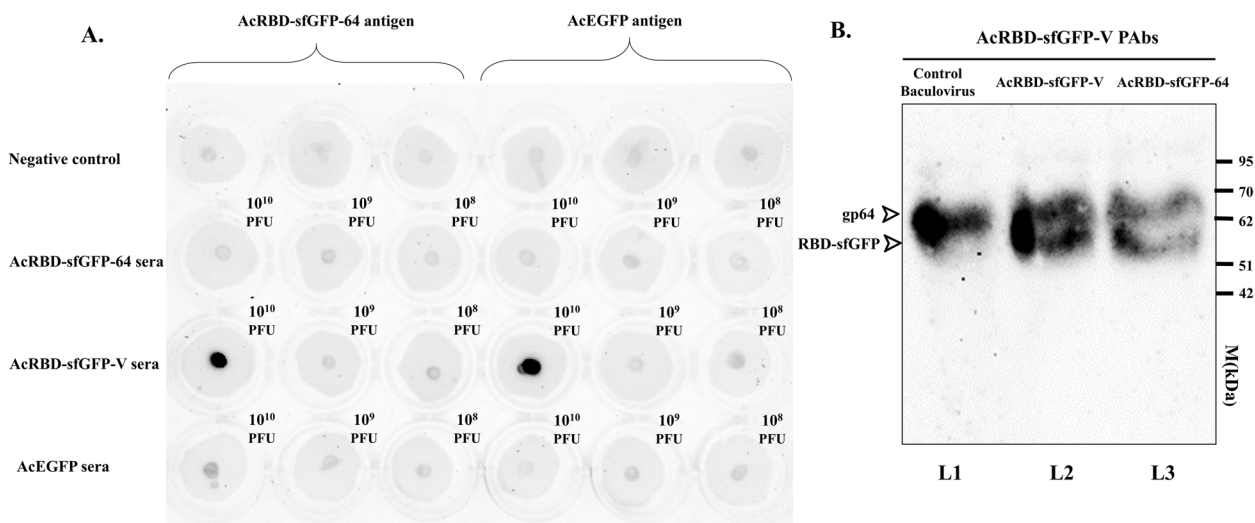


**Fig. 2** Production of polyclonal antibody by the pseudotyped virus from immunized BALB/C mice. **a** The virus displaying RBD produced antibodies that can bind both RBD and gp64 protein at  $10^{10}$  pfu/ml in a serum sample obtained from mice injected with AcRBD-sfGFP-V subcutaneously without any adjuvant. **b** Western blot of the AcRBD-sfGFP-64, AcRBD-sfGFP-V, and the AcDH10Bac detecting differences between the RBD-sfGFP and gp64 bands. Two distinguished bands corresponding to gp64 (~67 kDa) and RBD-sfGFP (~ 51 kDa) were observed in both AcRBD-sfGFP-64 and AcRBD-sfGFP-V samples but only a single band corresponding to gp64 was observed in the AcDH10Bac

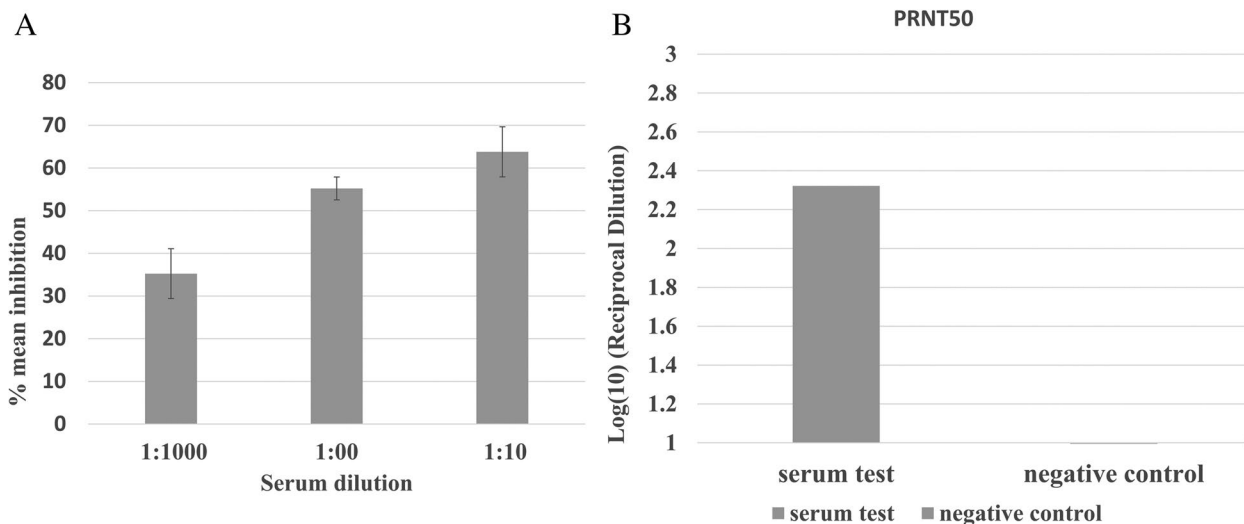


**Fig. 3** PRNT assay of the polyclonal antibodies produced by AcRBD-sfGFP-V immunization in BALB/C mice. **A** The bar chart shows the percent viral inhibition after 10-fold serial dilution. **B** A nonlinear relation is blotted and giving the equation  $y = -5.6833x^2 + 8.45x + 61.033$  where  $y$  substituted with 50 representing the neutralization titer (PRNT<sub>50</sub>) of SARS CoV-2 in Vero cells with PRNT<sub>50</sub> > 100 shown in the bar chart with respect to the negative control (no serum)

**AcRBD-sfGFP-V anti-sera inhibits an Egyptian wild-type isolate of SARS CoV-2 measured by PRNT**

This test is meant to examine the immunogenic ability of the produced PVs to produce mouse antibodies that can elicit neutralizing capability against the SARS-CoV-2 wild type. The obtained serum from mice injected with  $10^{10}$  PFU of AcRBD-sfGFP-V was 10-fold serial dilution of 1:10, 1:100, and 1:1000. The results revealed that

mice serum could reduce SARS-CoV-2 reproduction by approximately 30% at 1:1000, 50% at 1:100, and 70% at 1:10 (S2; Table. 2). Taking  $\text{Log}_{10}$  of the dilution reciprocal, the values 1, 2, and 3 represent 1:10, 1:100, and, 1:1000 respectively. Neutralization titer was determined between 100 and 200 as defined by the highest dilution that gives 50% inhibition (Fig. 3A, B).

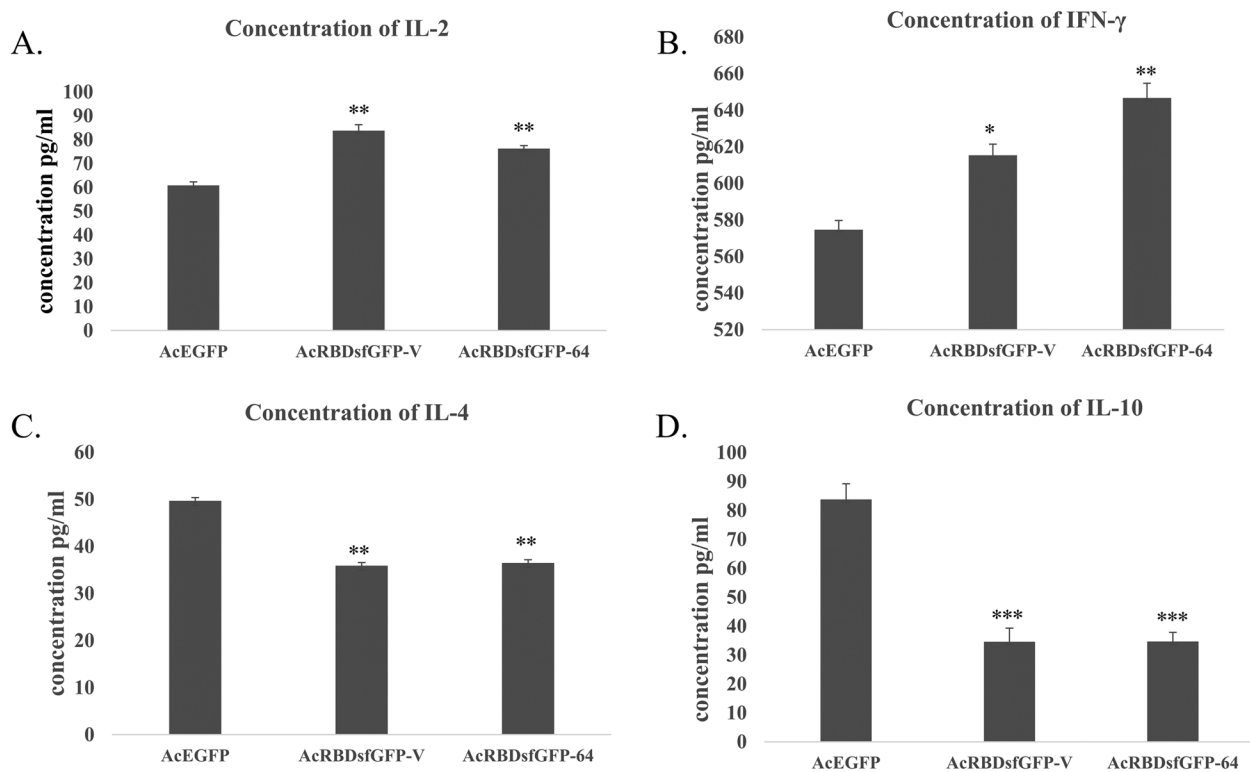


**Fig. 4** ELISA readings for splenic extracted cytokines show Th1 response in baculovirus displaying RBDsfGFP. **A** IL-2, **B** IFN- $\gamma$ , **C** IL-4, and **D** IL-10 in splenocytes of mice after injection with AcEGFP, AcRBDsfGFP-V, and AcRBDsfGFP-64. Data presented as mean  $\pm$  SD. \* $P$  value  $<0.05$ , \*\* $P$  value  $<0.01$ , and \*\*\* $P$  value  $<0.001$

#### AcRBD-sfGFP-V and AcRBD-sfGFP-64 increase the levels of IL-2 and IFN- $\gamma$ and decrease the levels of IL-4 and IL-10 in immunized mice

The preserved splenocytes were thawed and left overnight to attach; the cells count was between  $24 \times 10^6$ – $45 \times 10^6$ , and the viability was  $>90\%$ . The total protein extracted from the splenocytes was analyzed by ELISA ( $N=3$ ). The mean concentrations of IL-2 are 60.83 (SD=1.44), 83.75 (SD=2.5), and 76.25 (SD=1.25) for AcEGFP, AcRBD-sfGFP-V, and AcRBD-sfGFP-64, respectively. In parallel, INF gamma mean titers were 574.6 (SD=5), 615.3 (SD=6.1), 646.6 (SD=8) for AcEGFP, AcRBD-sfGFP-V, and AcRBD-sfGFP-64, respectively. On the other hand, the mean values for IL-4 were 49.7 (SD=0.95), 35.9 (SD=1.23), 36.5 (SD=0.66), and IL-10 83.8 (SD=5.3), 34.6 (SD=4.6), and 34.7 (SD=3.1) for AcEGFP, AcRBD-sfGFP-V, and AcRBD-sfGFP-64, respectively.

The results showed a significant increase ( $p < 0.01$ ) in the levels of IL-2 and IFN- $\gamma$  and a significant decrease ( $p < 0.01$ ) and ( $p < 0.001$ ) in IL-4 and IL10, respectively, of the isolated splenocytes from the immunized mice with AcRBD-sfGFP-V and AcRBD-sfGFP-64 compared to AcEGFP as shown in Fig. 4.

#### Discussion

One of the main challenges with pseudotyping is the balance between increasing membrane incorporation of the target protein and maintaining a high titer of the virus. This point was addressed carefully in our work. Usually, the choice of the promoter, the type of the fusion partner, and the nature of the protein structure dictate the efficiency of protein display. Even though early promoters of baculovirus are preferred for pseudotyping, the strong, very late polyhedrin promoter is highly efficient too [10]. Moreover, the distribution of the displayed protein is a crucial factor for the pseudotyped virus characteristics as it determines the binding affinity for cellular receptors. Previous work on baculovirus displayed a target protein with VSV-G (TM+CTD) in comparison with gp64 (TM+CTD). It was reported that from 2 to 7 displayed molecules mediated by VSV-G can be distributed symmetrically around the virus surface, but gp64 only presents fewer molecules on the apical ends when examined using the immunogold labeling technique [46]. Such a strategy was reported in baculovirus displaying SARS-CoV spike ectodomain successfully by VSV-G (TM+CTD) [47]. RBDsfGFP fusion will enable us to track the protein in the infected cell and detect it using

in-gel fluorescence and quantified by endpoint dilution. In contrast to GFP, sfGFP can tag membrane proteins to keep high-quality fluorescence [48, 49]. The results of in-gel fluorescence and endpoint dilution suggested that the fused RBD-sfGFP protein was efficiently displayed and did not negatively affect viral replication (Fig. 1c). Similarly, rabies virus envelope glycoprotein G was fused with the red fluorescence protein RFP and incorporated into the membrane to track virus particles in the entry process [50]. It is worth noting that purifying the viruses with the membrane ion-exchange chromatography method was efficient and did not alter the function of the displayed proteins according to the downstream experiments. The membrane ion-exchange chromatography method was done before; however, it was not tested for its impact on the displayed proteins with baculovirus [51].

The dot blot results confirmed that the VSV-G display is more efficient to trigger the immune response of BALB/C mice as seen in the intense bands of the concentration  $10^{10}$  PFU in contrast to the display using gp64 with the same dose (Fig. 2a). Moreover, the absence of gp64 strong signal may be explained by the decrease of the distribution of molecules in gp64 (TM+CTD) in contrast to VSV-G (TM+CTD) as mentioned before. In addition, western blot showed two intense bands around 64 and 51 kDa with the AcRBD-sGFP-V sample; the bands were more intense than with the AcRBD-sGFP-64 sample when tested with the serum from mice injected with AcRBD-sfGFP-V. Interestingly, in the control baculovirus lane, the intensity of the band corresponding to gp64 was nearly the same as with the AcRBD-sGFP-V lane. This may indicate that the numbers of the displayed protein mediated by VSV-G are more abundant than the ones mediated by gp64. In another work, the results of the western blot in baculovirus displaying SARS CoV-2 spike observed a drastic reduction when displayed by gp64 (TM+CTD) compared to VSV-G (TM+CTD); however, degradation products were observed with the displayed full spike and S1 subunit but not with the RBD alone probably due to the presence of specific protease [52]. Hence, it may be advisable to display smaller domains of the spike such as the RBD on baculovirus to prevent such modifications on the structure. Usually, the dose range  $10^8$ – $10^{10}$  PFU is recommended for eliciting the immune system as previously reported, which was within the range of our results [53–55]. Such different doses will depend on multi-factors such as the animal model, injection route, and adjuvant used. We have shown that a high dose of  $10^{10}$  can be enough to trigger the immune system without an adjuvant. This can be of great value to the economics of vaccines since the supply chain around the world has been affected especially in developing countries. The sole appearance of Gp64, in

addition to RBD, can be due to gp64 nature as it is the most abundant envelope protein. While the baculovirus BV envelope contains six more proteins other than gp64 [56]. These proteins are GP37 (Ac64), ODV-E25 (Ac94), ODV-E18 (Ac143), and BV/ODV-E26 (Ac16), F-like protein (Ac23), v-Ubi (Ac35) [55].

PRNT assay of the wild-type virus is a standard method indicating the efficacy of viral inhibition by neutralizing antibodies [57–59]. The value of PRNT50 is indicative of the strength of inhibition at a higher dilution. Our results show a PRNT50 value >100 after BALB/C immunization with  $10^{10}$  PFU of AcRBD-sfGFP-V injected subcutaneously (Fig. 3). The result was comparable to what was reported using baculovirus displaying Japanese encephalitis virus E glycoprotein with (PRNT50 = 1:115.2) [60]. Microneutralization assay of baculovirus displaying VP1 of Human Enterovirus 71 gave 1:32 to 1:64; however, mice were injected subcutaneously with a lower dose of 108 PFU but with Freund's adjuvant [54]. The display of Zika virus envelope protein on baculovirus with Freund's adjuvant after three doses gave PRNT50 = 1:47.76 after 15µg/dose intraperitoneal injection in mice [61]. These data indicate that our system can elicit comparable neutralizing antibodies compared to other displayed proteins on baculovirus displayed antigen. Interestingly, baculovirus expressed the full spike and gave high neutralizing titer while the S1 and RBD did not show significant neutralization [62]. Moreover, the Ad5 viral vector expressing SARS-CoV-2-S1 protein showed a microneutralization titer (NT90) value of about <40 [63]. Quite similar values were also reported in another viral vector vaccine with a lower dose and immunization period and both with a single dose injection [64]. Finally, it seems that the use of the trimeric or monomeric form of the recombinant vaccine is a matter of debate since the findings agree on the efficacy of monomeric and trimeric forms [65, 66].

The IL-2 and IFN- $\gamma$  were used as markers for the Th1 response shift. Both AcRBD-sfGFP-V and AcRBD-sfGFP-64 significantly increased IL-2 and IFN- $\gamma$ ; hence, this suggests that the displayed RBD induced Th1 response. Reduction in the concentration of IL-4 and IL-10 can result from the increased amount of INF- $\gamma$  interfering with IL-4 gene expression [67]. It is worth noting that Th1 response was achieved in several RBD-based vaccines as demonstrated in (Table 1). For instance, the addition of 3M052 adjuvant to the RBD subunit vaccine is suggested to induce dendritic cells to stimulate CD8+T cells specifically. It was reported that antibodies against the RBD did not show antibody-dependent enhancement (ADE) in vitro. For the current work, we confirmed some of the pros of using the RBD such as induction of the Th1 response, which was reported with several vaccine platforms instead of vaccines that induced Th2 biased CD4+

**Table 1** RBD-based vaccines with different formulations and the type of immune response that they trigger

Vaccine name	Developer	Dose timing	Clinical trials	Vaccine type	Used adjuvant	Immune response mechanism	Th1/Th2 immune balance	Reference
AiCov	Chinese Academy of Military Medical Sciences	0 and 28 days (100 µg)	Phase 1 clinical trial (ChiCTR2000034112)	mRNA encodes the SARS-CoV-2 RBD	Lipid nanoparticle encapsulated mRNA (mRNA-LNP)	Increase the level of CD4 <sup>+</sup> and CD8 <sup>+</sup> effector memory T cells, IFN-γ, TNF-α, and IL-2 in isolated splenocytes	Induce Th1 cellular immune response	[32]
BNT162b1	BioNTech and Pfizers	0 and 28 days (1–50 µg)	Phase 1 and 2 clinical trial	mRNA encodes the SARS-CoV-2 RBD	Lipid nanoparticle encapsulated mRNA (mRNA-LNP)	Elevation of CD4 <sup>+</sup> and CD8 <sup>+</sup> T cell responses and increase in the secretion of IFN-γ, IL-2, and IL-12p70	Induce Th1 cellular immune response	[33]
Folded RBD-PreS fusion vaccine	-	Three times in 3 weeks (20 or 40 µg)	-	SARS-CoV-2 RBD fused to the N- and C-terminus of hepatitis B virus (HBV) surface antigen PreS expressed in <i>E. coli</i> expression system	Aluminum hydroxide	Induce production of allergen-specific IgG responses (IgG1 and IgG 4)	-	[34]
ZF2001	Institute of Microbiology, Chinese Academy of Sciences, and Anhui Zhifei Longcom Biopharmaceutical	0, 30, and 60 days (25 µg per dose)	Phase 3 clinical trial	Adjuvant-based protein subunit vaccine	Aluminum hydroxide	Elevation of the levels of MHC class II-related genes, including cd74 and H2-Aa and induced the presentation of antigens to CD4 <sup>+</sup> T cells via MHCI molecules	Increase Th1 cytokine production (IFN-γ, IL-2) and Th2 cytokine production (IL-4) cytokine production resulting in Th1/Th2 balanced cytokines	[35, 36]
A yeast-expressed RBD-based SARS-CoV-2 vaccine	-	0, 4, and 9 weeks	-	Yeast expression system	3M-052-aluminum	Increase nAbs & elevation of CD4 <sup>+</sup> and CD8 <sup>+</sup> T cell responses	Induce Th1-biased CD4 <sup>+</sup> T cell reactions	[37]
Unnamed recombinant A2:8 vaccine	West China Hospital	0, 21 days and 0, 14, 28 days	Phase 2 clinical trial	The baculovirus expression system	Aluminum hydroxide gel	Increased levels of IgM and IgG in sera and increased the levels of IFN-γ and IL-4 from isolated lymphocytes	Enhanced and TH1/TH2 balanced cytokine production	[38]
Mutant RBD vaccines	-	0 and 14 days	-	HIV-1 backbone	Aluminum	High geometric mean titers (GMTs) of neutralizing antibodies (nAbs)	-	[39]

T cell responses that aggravate respiratory diseases as reported before [32–39].

## Conclusions

In this study, we confirmed that SARS CoV-2 pseudotyped baculovirus can effectively display the RBD and maintain functionality by producing neutralizing antibodies against SARS CoV-2 local isolate in Egypt (hCoV-19/Egypt/NRC-03/2020). Our preliminary data support that baculovirus-based RBD display could be a safe and effective approach as a vaccine. In addition, dose 1010 PFU without adjuvant is highly recommended due to its safety and efficacy in BALB/C mice. Such results are very promising for further investigations into display-based vaccines. Indeed, we faced some limitations such as inaccessibility to animals for a challenging study and overall biosafety level three and inability to test new variants as well. However, we were interested to study the baculovirus as a platform for RBD display with emphasis on its adjuvant effect, safety, and Th1/Th2 response balance. Overall, the model can help immunologists to study its efficacy as a safe vaccine.

## Abbreviations

SARS CoV-2	Severe acute respiratory syndrome coronavirus 2
RBD	Receptor-binding domain
PRNT	Plaque reduction neutralization test
GP64	Glycoprotein 64
VSV-G	Vesicular stomatitis virus glycoprotein G
AcMNPV	<i>Autographa californica</i> multiple nucleopolyhedrovirus
NT90	Neutralization titer 90
NT50	Neutralization titer 50
PFU	Particle-forming unit
TCID	Tissue culture infectious dose
MOI	Multiplicity of infection
sfGFP	Superfolder green fluorescent protein
MD	Mature domain
CTD	C-terminal domain
TM	Transmembrane

## Supplementary Information

The online version contains supplementary material available at <https://doi.org/10.1186/s43141-023-00472-2>.

**Additional file 1: Table S1.** Vaccines are adopted in several systems and have different immune responses.

**Additional file 2: Table S2.** PRNT results indicated by viral inhibition percentage in three 10-fold dilutions. The 10-fold serially diluted serum shows a decrease in SARS-CoV-2 reproduction in Vero cells with a minimum of 30% inhibition after 1:1000 serum dilution and more than 71% after 1:10 serum dilution.

**Additional file 3.** Sequencing results of the clone AcrBD-sfGFP-V. >pFast-DualsvgtMSS RPDGFP\_pFASTBAC-R-5HD372-11108153806.

**Additional file 4.** S4\_ELISA plate reader raw dataR1.

## Acknowledgements

We would like to thank Dr. Ahmed Abdelsamea for helping with the statistical analysis. We would like to extend our thanks to Dr. Marwan Emara and Dr. Menna El-Serafy for their help and support in using the CAAD and GC facilities.

## Author's contributions

Conceptualization, T.Z.S., M.A.W., and D.M.; data curation, M.A.W.; formal analysis, T.Z.S. and M.A.W.; investigation, M.A.W., D.M., D.A.G., and J.I.O.; methodology, T.Z.S., M.A.W., D. M., and D.A.G.; resources, M.A.W., D.M., and D.A.G.; visualization, M.A.W., and J.I.O.; writing—original draft, M.A.W.; writing—review and editing, T.Z.S., M.A.W., D.M., and J.I.O.; project administration, T.Z.S.; supervision, T.Z.S.; and funding acquisition, T.Z.S. The authors read and approved the final manuscript.

## Funding

This work is supported by the Academy of Scientific Research and Technology (ASRT) (grant No.:ASRT 7222) and the Science, Technology & Innovation Funding Authority (STDF) (grant No: STIFA 45396).

## Availability of data and materials

Not applicable.

## Declarations

### Ethics approval and consent to participate

The research involves animal experiments. The mice were treated in accordance with the guidelines and policies of the National Institute of Health (NIH) animal care. All experiments were approved by the research ethics committee (IACUC#50-25-1121) issued from the Pharmaceutical & Fermentation Industries Development Center, SRTA-City, Egypt.

### Consent for publication

Not applicable.

### Competing interests

The authors declare that they have no competing interests.

Received: 4 September 2022 Accepted: 26 January 2023

Published online: 09 February 2023

## References

- Howard C, Fletcher N (2012) Emerging virus diseases: can we ever expect the unexpected? *Emerg Microbes Infect* 1(1):1–9. <https://doi.org/10.1038/emi.2012.47>
- Naeem W, Zeb H, Rashid M (2022) Laboratory biosafety measures of SARS-CoV-2 at containment level 2 with particular reference to its more infective variants. *Biosafe Health* 4(1):11–14. <https://doi.org/10.1016/j.bshealth.2021.12.005>
- Kiener T, Premanand B, Kwang J (2013) Immune responses to baculovirus-displayed enterovirus 71 VP1 antigen. *Expert Rev Vaccines* 12(4):357–364
- Ritchie H. E, Mathieu L, Rodés-Guirao C, Appel C, Giattino E, Ortiz-Ospina J, Hasell B, Macdonald D, Roser M. Coronavirus (COVID-19) Vaccinations. 2020. Available online: <https://ourworldindata.org/covid-vaccinations> (Accessed on 12 May 2022)
- Salem T, Zhang F, Sahly N, Thiem S (2018) Effect of temporal expression of integral membrane proteins by baculovirus expression vector system. *Mole Biotechnol* 60(8):576–584
- Ayres MD, Howard SC, Lopez-Ferber M, Lopez-Ferber M, Possee RD (1994) The complete DNA sequence of *Autographa californica* nuclear polyhedrovirus. *Virology* 202(2):586–605. <https://doi.org/10.1006/VIRO.1994.1380>
- Madhan S, Prabakaran M, Kwang J (2010) Baculovirus as vaccine vectors. *Current Gene Therapy* 10(3):201–213. <https://doi.org/10.2174/156652310791321233>
- Airenne KJ, Makkonen K, Mähönen AJ, Ylä-Herttuala S (2010) In vivo application and tracking of baculovirus. *Current Gene Therapy* 10(3):187–194. <https://doi.org/10.2174/156652310791321206>
- Hu L, Li Y, Ning Y, Deng F, Vlak J, Hu Z et al (2019) The major hurdle for effective baculovirus transduction into mammalian cells is passing early endosomes. *J Virol* 93(15). <https://doi.org/10.1128/jvi.00709-19>
- Chen CY, Lin CY, Chen GY, Hu YC (2011) Baculovirus as a gene delivery vector: recent understandings of molecular alterations in transduced

- cells and latest applications. *Biotechnol Adv* 29(6):618–631. <https://doi.org/10.1016/J.BIOTECHADV.2011.04.004>
11. Kitagawa Y, Tani H, Limn C, Matsunaga T, Moriishi K, Matsuura Y (2005) Ligand-directed gene targeting to mammalian cells by pseudotype baculoviruses. *J Virol* 79(6):3639–3652. <https://doi.org/10.1128/jvi.79.6.3639-3652.2005>
  12. Grabherr R, Ernst W, Doblhoff-Dier O, Sara M, Katinger H (1997) Expression of foreign proteins on the surface of *Autographa californica* nuclear polyhedrosis virus. *Biotechniques* 22(4):730–735. <https://doi.org/10.2144/97224rr02>
  13. Oker-Blom C, Airene K. J, Grabherr R. Baculovirus display strategies: emerging tools for eukaryotic libraries and gene delivery. *Brief Funct Genom* 2003; 2(3), 244–253. <https://doi.org/10.1093/BFGP/2.3.244>
  14. Kaikkonen M, Rätty J, Airene K, Wirth T, Heikura T, Ylä-Herttua S (2006) Truncated vesicular stomatitis virus G protein improves baculovirus transduction efficiency in vitro and in vivo. *Gene Therapy* 13(4):304–312. <https://doi.org/10.1038/sj.gt.3302657>
  15. Romanowski V (2013) Current issues in molecular virology - viral genetics and biotechnological applications. IntechOpen, London, p 296. [cited 2022 May 12]. Available from: <https://www.intechopen.com/books/3505>. <https://doi.org/10.5772/50089>
  16. Abe T, Hemmi H, Miyamoto H, Moriishi K, Tamura S, Takaku H, Akira S, Matsuura Y (2005) Involvement of the Toll-like receptor 9 signaling pathway in the induction of innate immunity by baculovirus. *J Virol* 79(5):2847–2858
  17. Abe T, Takahashi H, Hamazaki H, Miyano-Kurosaki N, Matsuura Y, Takaku H (2003) Baculovirus induces an innate immune response and confers protection from lethal influenza virus infection in mice. *J Immunol* 171(3):1133–1139
  18. Chen C, Liu H, Tsai C, Chung C, Shih Y, Chang P et al (2010) Baculovirus as an avian influenza vaccine vector: differential immune responses elicited by different vector forms. *Vaccine*. 28(48):7644–7651
  19. Pieroni L, Maione D, La Monica N (2001) *<i>In Vivo</i>* Gene transfer in mouse skeletal muscle mediated by baculovirus vectors. *Human Gene Therapy*. 12(8):871–881
  20. Choi J, Gwon Y, Kim J, Cho Y, Heo Y, Cho H et al (2013) Protective efficacy of a human endogenous retrovirus envelope-coated, nonreplicable, baculovirus-based Hemagglutinin vaccine against pandemic influenza H1N1 2009. *PLoS ONE*. 8(11):e80762
  21. Su S, Wong G, Shi W, Liu J, Lai A, Zhou J et al (2016) Epidemiology, genetic recombination, and pathogenesis of coronaviruses. *Trends Microbiol* 24(6):490–502. <https://doi.org/10.1016/j.tim.2016.03.003>
  22. Zhu N, Zhang D, Wang W, Li X, Yang B, Song J et al (2020) A novel coronavirus from patients with pneumonia in China; 2019. *New Engl J Med* 382(8):727–733. <https://doi.org/10.1056/nejmoa2001017>
  23. Jackson C, Farzan M, Chen B, Choe H (2021) Mechanisms of SARS-CoV-2 entry into cells. *Nat Rev Molecular Cell Biology* 23(1):3–20. <https://doi.org/10.1038/s41580-021-00418-x>
  24. Freund NT, et al (2015) Reconstitution of the receptor-binding motif of the SARS coronavirus, *Protein Eng Design Sel* 28(12):567–575. Available at: <https://doi.org/10.1093/protein/gzv052>
  25. Almuqrin A, et al (2021) SARS-COV-2 vaccine ChAdOx1 nCoV-19 infection of human cell lines reveals low levels of viral backbone gene transcription alongside very high levels of SARS-COV-2 s glycoprotein gene transcription, *Genome Med* 13(1). Available at: <https://doi.org/10.1186/s13073-021-00859-1>
  26. Kowarz E, Krutzke L, Reis J, Bracharz S, Kochanek S, Marschalek R (2021) Vaccine-Induced COVID-19 Mimicry Syndrome: Splice reactions within the SARS-CoV-2 Spike open reading frame result in Spike protein variants that may cause thromboembolic events in patients immunized with vector-based vaccines
  27. Greinacher A, Thiele T, Warkentin T, Weisser K, Kyrle P, Eichinger S (2021) Thrombotic thrombocytopenia after ChAdOx1 nCov-19 vaccination. *New England J Med* 384(22):2092–2101
  28. Heinz FX, Stiasny K (2021) "Distinguishing features of current COVID-19 vaccines: Knowns and unknowns of antigen presentation and modes of action," *npj Vaccines* 6(1). Available at: <https://doi.org/10.1038/s41541-021-00369-6>
  29. Valdes-Balbin Y, Santana-Mederos D, Quintero L, Fernández S, Rodriguez L, Sanchez Ramirez B et al (2021) SARS-CoV-2 RBD-tetanus toxoid conjugate vaccine induces a strong neutralizing immunity in preclinical studies. *ACS Chem Biol* 16(7):1223–1233
  30. Liang Z, et al (2020) Adjuvants for coronavirus vaccines. *Front Immunol* 11. Available at: <https://doi.org/10.3389/fimmu.2020.589833>
  31. Schmidt T, Klemis V, Schub D, Schneitler S, Reichert M, Wilkens H, Sester U, Sester M, Mihm J (2021) Cellular immunity predominates over humoral immunity after homologous and heterologous mRNA and vector-based COVID-19 vaccine regimens in solid organ transplant recipients. *Am J Transplant* 21(12):3990–4002
  32. Zhang N-N, Li X-F, Deng Y-Q, Zhao H, Huang Y-J, Yang G et al (2020) A thermostable mRNA vaccine against COVID-19. *Cell* 182:1271–1283.e16. <https://doi.org/10.1016/j.cell.2020.07.024>
  33. Sahin U, Muik A, Derhovanessian E, Vogler I, Kranz LM, Vormehr M et al (2020) COVID-19 vaccine BNT162b1 elicits human antibody and TH1 T cell responses. *Nature* 586:594–599. <https://doi.org/10.1038/s41586-020-2814-7>
  34. Gattinger P, Kratzer B, Tulaeva I, Niespodziana K, Ohradnova-Repic A, Gebetsberger L et al (2022) Vaccine based on folded RBD-PreS fusion protein with potential to induce sterilizing immunity to SARS-CoV-2 variants. *Allergy*. <https://doi.org/10.1111/all.15305>
  35. Wang Q, Song Z, Yang J, He Q, Mao Q, Bai Y et al (2022) Transcriptomic analysis of the innate immune signatures of a SARS-CoV-2 protein subunit vaccine ZF2001 and an mRNA vaccine RRV. *Emerg Microbes Infect* 11(11):1145–1153. <https://doi.org/10.1080/22221751.2022.2059404>
  36. An Y, Li S, Jin X, Han J, Xu K, Xu S et al (2022) A tandem-repeat dimeric RBD protein-based COVID-19 vaccine zf2001 protects mice and nonhuman primates. *Emerg Microbes Infect* 11(1):1058–1071. <https://doi.org/10.1080/22221751.2022.2056524>
  37. Pino M, Abid T, Pereira Ribeiro S, Edara V, Floyd K, Smith J et al (2021) A yeast-expressed RBD-based SARS-CoV-2 vaccine formulated with 3M-052-alum adjuvant promotes protective efficacy in non-human primates. *Sci Immunol* 6(61). <https://doi.org/10.1126/sciimmunol.abh3634>
  38. Yang J, Wang W, Chen Z, Lu S, Yang F, Bi Z et al (2020) A vaccine targeting the RBD of the S protein of SARS-CoV-2 induces protective immunity. *Nature* 586:572–577. <https://doi.org/10.1038/s41586-020-2599-8>
  39. Song S, Zhou B, Cheng L, Liu W, Fan Q, Ge X et al (2022) Sequential immunization with SARS-CoV-2 RBD vaccine induces potent and broad neutralization against variants in mice. *Virology* 19(1). <https://doi.org/10.1186/s12985-021-01737-3>
  40. Lyons-Weiler J (2020) Pathogenic priming likely contributes to serious and critical illness and mortality in COVID-19 via autoimmunity. *J Transl Autoimmun* 3:100051
  41. Chan K, Dorosky D, Sharma P, Abbasi S, Dye J, Kranz D, Herbert A, Procko E (2020) Engineering human ACE2 to optimize binding to the spike protein of SARS coronavirus 2. *Science* 369(6508):1261–1265
  42. Abdelhamid H, Salem T Z, Wahba MA, Mofed D, Morsy OE, Abdelbaset R (2022) A capacitive sensor for differentiation between virus-infected and uninfected cells. *Sensing Bio Sensing Res* 36:100497. <https://doi.org/10.1016/j.bsrs.2022.100497>
  43. O'Reilly D, Miller L, Luckow V. Baculovirus expression vectors. In Oxford University Press 1994. New York USA. [https://doi.org/10.1016/0167-7799\(93\)90146-z](https://doi.org/10.1016/0167-7799(93)90146-z)
  44. Salem TZ, Zhang F, Thiem SM (2013) Reduced expression of *Autographa californica* nucleopolyhedrovirus ORF34, an essential gene, enhances heterologous gene expression. *Virology* 435(2):225–238. <https://doi.org/10.1016/j.virol.2012.10.022>
  45. Hayden F, Cote K, Douglas R (1980) Plaque inhibition assay for drug susceptibility testing of influenza viruses. *Antimicrobial Agents Chemother* 17(5):865–870. <https://doi.org/10.1128/aac.17.5.865>
  46. Ojala K, Koski J, Ernst W, Grabherr R, Jones I, Oker-Blom C (2004) Improved display of synthetic IgG-binding domains on the baculovirus surface. *Technol Cancer Res Treat* 3(1):77–84. <https://doi.org/10.1177/153303460400300109>
  47. Feng Q, Liu Y, Qu X, Deng H, Ding M, Lau T et al (2006) Baculovirus surface display of SARS coronavirus (SARS-CoV) spike protein and immunogenicity of the displayed protein in mice models. *DNA Cell Biol* 25(12):668–673. <https://doi.org/10.1089/dna.2006.25.668>
  48. Feilmeier B, Iseminger G, Schroeder D, Webber H, Phillips G (2000) Green fluorescent protein functions as a reporter for protein localization in

- Escherichia coli. *J Bacteriol* 182(14):4068–4076. <https://doi.org/10.1128/jb.182.14.4068-4076.2000>
49. Dinh T, Bernhardt T (2011) Using superfolder green fluorescent protein for periplasmic protein localization studies. *J Bacteriol* 193(18):4984–4987. <https://doi.org/10.1128/jb.00315-11>
  50. Kligen Y, Conzelmann KFinke S. (2008) Double-labeled rabies virus: live tracking of enveloped virus transport. *J Virol* 82(1):237–245. <https://doi.org/10.1128/JVI.01342-07>
  51. Grein T, Michalsky R, Vega López M, Czernak P (2012) Purification of a recombinant baculovirus of *Autographa californica* M nucleopolyhedrovirus by ion exchange membrane chromatography. *J Virol Methods* 183(2):117–124. <https://doi.org/10.1016/j.jviromet.2012.03.031>
  52. Wang L, Zhao L, Li Y, Ma P, Kornberg R, Nie Y (2022) Harnessing coronavirus spike proteins' binding affinity to ACE2 receptor through a novel baculovirus surface display system. *Biochem Biophys Res Commun* 606:23–28. <https://doi.org/10.1016/j.bbrc.2022.03.062>
  53. Facciabene A, Aurisicchio L, La Monica N (2004) Baculovirus vectors elicit antigen-specific immune responses in mice. *J Virol* 78(16):8663–8672. <https://doi.org/10.1128/jvi.78.16.8663-8672.2004>
  54. Meng T, Kolpe A, Kiener T, Chow V, Kwang J (2011) Display of VP1 on the surface of baculovirus and its immunogenicity against heterologous human enterovirus 71 strains in mice. *Plos ONE* 6(7):e21757. <https://doi.org/10.1371/journal.pone.0021757>
  55. Blissard G, Theilmann D (2018) Baculovirus entry and egress from insect cells. *Ann Rev Virol* 5(1):113–139. <https://doi.org/10.1146/annurev-virol-092917-043356>
  56. Wang R, Deng F, Hou D, Zhao Y, Guo L, Wang H, Hu Z (2010) Proteomics of the *Autographa californica* Nucleopolyhedrovirus Budded Virions. *J Virol* 84(14):7233–7242. <https://doi.org/10.1128/jvi.00040-10>
  57. Campi-Azevedo A, Peruhype-Magalhães V, Coelho-dos-Reis J, Antonelli L, Costa-Pereira C, Speziali E et al (2019) 17DD yellow fever revaccination and heightened long-term immunity in populations of disease-endemic areas, Brazil. *Emerg Infect Dis* 25(8):1511–1521. <https://doi.org/10.3201/eid2508.181432>
  58. Cohen B, Doblas D, Andrews N (2008) Comparison of plaque reduction neutralisation test (PRNT) and measles virus-specific IgG ELISA for assessing immunogenicity of measles vaccination. *Vaccine* 26(50):6392–6397. <https://doi.org/10.1016/j.vaccine.2008.08.074>
  59. Eyal O, Olshevsky U, Lustig S, Paran N, Halevy M, Schneider P et al (2005) Development of a tissue-culture-based enzyme-immunoassay method for the quantitation of anti-vaccinia-neutralizing antibodies in human sera. *J Virol Methods* 130(1-2):15–21. <https://doi.org/10.1016/j.jviromet.2005.05.027>
  60. Xu X, Wang Z, Zhang Q, Li Z, Zhao H, Li W et al (2011) Baculovirus surface display of E envelope glycoprotein of Japanese encephalitis virus and its immunogenicity of the displayed proteins in mouse and swine models. *Vaccine* 29(4):636–643. <https://doi.org/10.1016/j.vaccine.2010.11.045>
  61. Luo D, Miao Y, Ke X, Tan Z, Hu C, Li P et al (2020) Baculovirus surface display of Zika virus envelope protein protects against virus challenge in mouse model. *Virologica Sinica* 35(5):637–650. <https://doi.org/10.1007/s12250-020-00238-x>
  62. Cho H, Jang Y, Park K, Choi H, Nowakowska A, Lee H et al (2021) Human endogenous retrovirus-enveloped baculoviral DNA vaccines against MERS-CoV and SARS-CoV2. *Npj Vaccines* 6(1). <https://doi.org/10.1038/s41541-021-00303-w>
  63. Kim E, Weisel F, Balmert S, Khan M, Huang S, Erdos G et al (2021) A single subcutaneous or intranasal immunization with adenovirus-based SARS-CoV-2 vaccine induces robust humoral and cellular immune responses in mice. *Eur J Immunol* 51(7):1774–1784. <https://doi.org/10.1002/eji.202149167>
  64. Wu S, Zhong G, Zhang J, Shuai L, Zhang Z, Wen Z et al (2020) A single dose of an adenovirus-vectored vaccine provides protection against SARS-CoV-2 challenge. *Nat Commun* 11(1). <https://doi.org/10.1038/s41467-020-17972-1>
  65. van Vuren J, Petrus AJ, McAuley MJ, Kuiper NB, Singanallur MP, Bruce SR, Goldie S et al (2022) Highly thermotolerant SARS-Cov-2 vaccine elicits neutralising antibodies against delta and omicron in mice. *Viruses* 14(4):800. <https://doi.org/10.3390/v14040800>
  66. Routhu N, Cheedarla N, Bollimpelli V, Gangadhara S, Edara V, Lai L et al (2021) SARS-CoV-2 RBD trimer protein adjuvanted with Alum-3M-052 protects from SARS-CoV-2 infection and immune pathology in the lung. *Nat Commun* 12(1). <https://doi.org/10.1038/s41467-021-23942-y>
  67. Elser B et al (2002) IFN- $\gamma$  represses IL-4 expression via IRF-1 and IRF-2. *Immunity* 17(6):703–712. [https://doi.org/10.1016/s1074-7613\(02\)00471-5](https://doi.org/10.1016/s1074-7613(02)00471-5)

## Publisher's Note

Springer Nature remains neutral with regard to jurisdictional claims in published maps and institutional affiliations.

Submit your manuscript to a SpringerOpen® journal and benefit from:

- Convenient online submission
- Rigorous peer review
- Open access: articles freely available online
- High visibility within the field
- Retaining the copyright to your article

Submit your next manuscript at ► [springeropen.com](https://www.springeropen.com)